Electron-trapping centers and interstitials in chlorinated $SrCl_2$:Fe single crystals

D. Ghica and S. V. Nistor
National Institute for Materials Physics, POB MG-7 Magurele, RO-77125 Bucharest, Romania

E. Goovaerts and D. Schoemaker
Physics Department - CDE, University of Antwerp, Universiteitsplein 1, BE-2610 Antwerpen (Wilrijk), Belgium

H. Vrielinck and F. Callens
Department of Solid State Sciences, Ghent University, Krijgslaan 281 - S1, BE-9000 Ghent, Belgium
(Received 12 January 2006; revised manuscript received 17 March 2006; published 1 May 2006)

Electron-trapped Fe^+-type centers, produced by x-ray irradiation at 80 K and further annealing at higher temperatures in iron-doped $SrCl_2$ single crystals grown in chlorine gas, have been investigated by electron paramagnetic resonance. The Fe^+(III) and Fe^+(IIIa) centers, produced by annealing at temperatures higher than 200 K, exhibit monoclinic local symmetry with the two $\tilde{g}$- tensor principal axes situated in the (110) plane slightly tilted away from the [001] and [1–10] directions, respectively. The Fe^+(IV) center, observed after several cycles of irradiation and annealing to 700 K, exhibits tetragonal local symmetry around ⟨100⟩ and a well-resolved four-component structure, attributed to the superhyperfine interaction with a neighboring monovalent impurity ion. The presence and properties of the low symmetry radiation-induced Fe^+ paramagnetic centers are attributed to trapping and the thermally activated movement of chlorine interstitials. Both precursor Fe^{2+} and resulting Fe^+ centers are perturbed by these interstitials, which are introduced in $SrCl_2$:Fe crystals during growth under a chlorine atmosphere.

DOI: 10.1103/PhysRevB.73.174103 PACS number(s): 61.72.Ji, 61.80.Cb, 76.30.Fc

I. INTRODUCTION

Iron enters the $SrCl_2$ host lattice (cubic—O_h^5—fluorite structure) as Fe^{2+} impurity ions, which are difficult to observe by electron paramagnetic resonance (EPR) spectroscopy due to their $d^6(^5D)$ ground state.[1] One expects the electrons and holes produced by ionizing radiation to be trapped at the Fe^{2+} impurity ions situated at unperturbed substitutional Sr^{2+} cation sites. The resulting Fe^+ and Fe^{3+} paramagnetic centers, respectively, would therefore exhibit cubic symmetry. Indeed, a hole-trapped cubic Fe^{3+} center, called Fe^{3+}_{cub}, has been observed in early EPR measurements on $SrCl_2$:Fe crystals which were grown in an inert atmosphere and x-ray irradiated at room temperature (RT).[2] No electron-trapped Fe^+ centers have been reported so far in such crystals, which might be due to their intrinsic instability.

As previously observed in the case of iron-doped alkali chloride crystals grown in a chlorine atmosphere (chlorinated),[3] new electron and hole trapped centers are also produced with ionizing radiation of chlorinated $SrCl_2$ crystals doped with iron. It was found[4–8] that in such crystals the Fe^{2+} impurity ions can trap both electrons and holes, resulting in Fe^+ and Fe^{3+} paramagnetic centers both with noncubic symmetry. One could thus identify after x-ray irradiation at 80 K the following new paramagnetic centers: A hole-trapped Fe^{3+} center with local ⟨111⟩ trigonal symmetry,[4] called Fe^{3+}_{trig}, two electron-trapped centers, Fe^+(I) and Fe^+(II) with local ⟨001⟩ tetragonal symmetry,[5] as well as an electron-trapped center, called Fe^+(IIa), with local monoclinic symmetry.[8] Because the resulting Fe-related centers were produced after short irradiation at $T<100$ K, where no significant ionic movement is present,[9,10] it is expected that precursor Fe^{2+} centers with similar structure/symmetry are present in the as-grown crystal.

Such observations strongly suggest that chlorination induces precursor Fe^{2+} centers, with the iron impurity localized at other noncubic lattice sites. In an attempt to better understand the steric configurations of the Fe^{2+} precursors in the $SrCl_2$ crystal lattice, as well as the properties of the resulting electron/hole trapped Fe^+/Fe^{3+} centers, we have investigated thermally induced changes in the EPR spectra of the low-temperature-irradiated $SrCl_2$:Fe crystals.

As will be shown in this paper, the annealing of such low-temperature-irradiated $SrCl_2$:Fe crystals results in the formation of electron-trapped Fe^+ centers, which have been investigated by EPR. These results allow for a better understanding of the various Fe^{2+} center structures in the $SrCl_2$ crystal lattice and the localization of excess chlorine in the as-grown crystals. Moreover, the chlorine interstitials are shown to play an important role in the formation of iron-related electron and hole trapping centers.

II. EXPERIMENT

All samples used in this work were cleaved with the long edge along a crystal ⟨110⟩ direction from the same $SrCl_2$:Fe single-crystal ingots, grown by the Bridgman technique in a chlorine atmosphere, which were employed in the previous studies.[4–8] Typical sample sizes were $3\times3\times10$ mm^3 in the X band and $1\times1\times5$ mm^3 in the Q band. The samples were irradiated with x rays (W anode operating at 50 mA and 50 kV) at $T=80$ K for 30 min and further transferred in the microwave cavity without warming them up above 100 K.

The X-band EPR measurements were performed with a BRUKER ESP300E spectrometer, equipped with a gas-flow

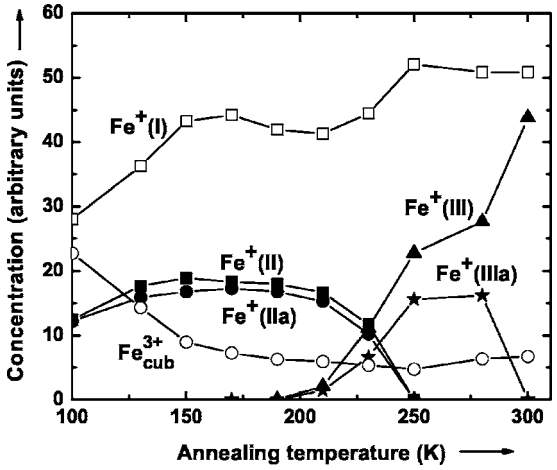

FIG. 1. Thermal growth/decay of the electron and hole trapped centers in chlorinated $SrCl_2$:Fe crystals, x-ray irradiated at 80 K, and measured at $T=3.5$ K. Only the relative concentration of the cubic Fe^{3+} center is given. The concentration of the Fe^{3+}_{trig} (not shown) does not change significantly in this temperature region.

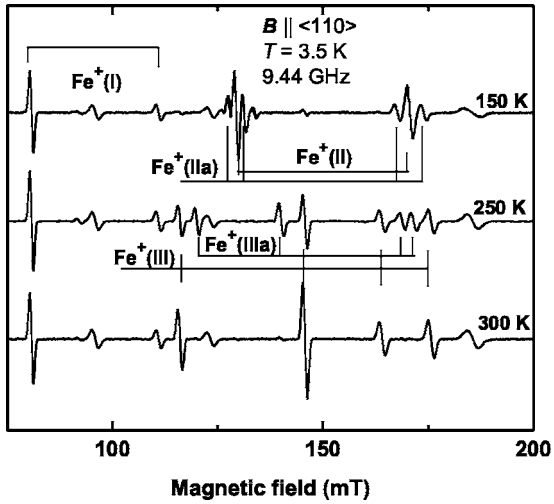

FIG. 2. X-band EPR spectra of a chlorinated $SrCl_2$:Fe crystal x-ray irradiated at 80 K and annealed at 150 K, 250 K, and 300 K, respectively. The unmarked transitions correspond to the Fe^{3+}_{trig} center.

cryogenic system for operation in the temperature range from 1.5 to 293 K. The Q-band EPR spectra were recorded using a BRUKER ELEXSYS E500 spectrometer, equipped with an Oxford CF935 gas-flow cryostat operating in the same temperature range.

III. RESULTS

A. Pulse annealing experiments

The thermal growth and decay of the electron and hole trapped centers in chlorinated $SrCl_2$:Fe crystals x-ray irradiated at 80 K have been investigated by pulse annealing experiments. In all experiments, the sample, which was previously x-ray irradiated at $T=80$ K and transferred in the microwave cavity with minimum warming up, was heated to the annealing temperature for 5 min and recooled to the same EPR measuring temperature ($T=3.5$ K). The evolution of the total EPR line intensities of each type of observed electron-trapped Fe^+ center ($S_{eff}=1/2$), determined for the $B\|\langle 110\rangle$ orientation, which is proportional to its concentration, is presented in Fig. 1, as a function of the annealing temperature. In the same figure, only the relative concentration of the cubic Fe^{3+} ($S=5/2$ ground state) centers is presented in order to illustrate the defects formation/annealing kinetics. The concentration of the Fe^{3+}_{trig} centers, which did not exhibit significant changes in the whole temperature range, has not been included in the figure.

The experiments show that both Fe^+(II) and Fe^+(IIa) centers exhibit similar temperature stability and concentration, which initially increases with the annealing temperature. They reach a maximum concentration around 150 K. Both centers begin to decay above 190 K and completely disappear at 250 K. Their decay is accompanied by the growth of some EPR lines (Fig. 2) attributed to two other paramagnetic centers, called Fe^+(III) and Fe^+(IIIa). The Fe^+(III) and Fe^+(IIIa) centers exhibit, up to approximately 280 K, similar annealing behavior. At higher temperatures, the decay of the Fe^+(IIIa) centers is accompanied (Fig. 2) by a further comparable increase in the concentration of the Fe^+(III) centers, which are stable at RT.

The EPR properties of the Fe^+(III) and Fe^+(IIIa) centers have been investigated in the hope that, together with the results of the annealing experiments, one could obtain a better insight into their structure and transformation mechanisms, as well as that of the related Fe^+-type centers.

B. EPR properties of the Fe^+(III) and Fe^+(IIIa) centers

As previously mentioned, the $SrCl_2$:Fe crystals which have been x-ray irradiated at $T=80$ K and annealed at RT exhibit at $T<15$ K, in addition to the EPR lines of the already studied Fe^+(I), Fe^{3+}_{cub} and Fe^{3+}_{trig} centers,[2,4,5] intense lines (Fig. 3). These lines, attributed to a paramagnetic center called Fe^+(III), exhibit strong temperature dependence, being hardly visible for $T\geqslant 15$ K. At $T<5$ K, the EPR lines are comparable in intensity with those of the Fe^+(I) center, beginning to saturate at microwave powers of about 4 mW.

With the magnetic field rotated in a {110} plane, the EPR spectrum of the Fe^+(III) centers consists of up to seven lines, some of them degenerate. From their intensity ratios, it can be assumed that the number of equivalent paramagnetic species is 12, and the local symmetry of the center is monoclinic (point symmetry $2/m^3$ in a m3m cubic crystal).[11]

The observed angular variation of the X-band EPR spectrum, as recorded in a {110} plane, is represented by full circles in Fig. 3(b). The solid lines represent the simulation based on a least-squares $\vec{\vec{g}}$-tensor fitting to the experimental data, using the spin Hamiltonian with effective spin $S=1/2$ and monoclinic $\vec{\vec{g}}$[1]

$$\hat{H}_S = \mu_B \vec{B} \cdot \vec{\vec{g}} \cdot \hat{S}. \quad (1)$$

A very good fitting was obtained with the spin Hamiltonian parameters given in Table I.

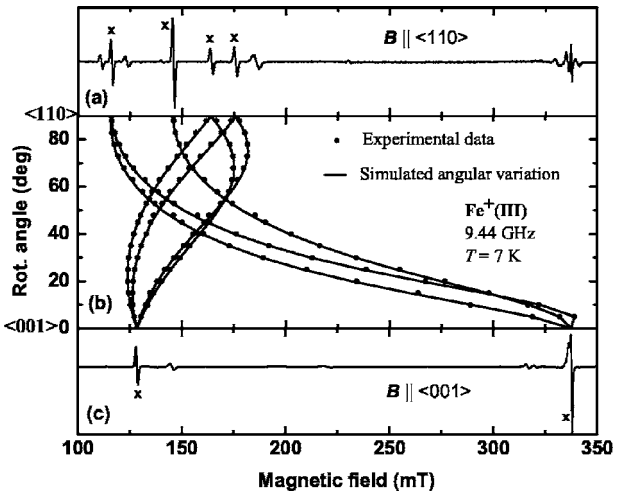

FIG. 3. X-band EPR spectra of a chlorinated $SrCl_2$:Fe crystal x-ray irradiated at 80 K and annealed for 5 min at RT, for $\boldsymbol{B}\|\langle 110\rangle$ in (a) and $\boldsymbol{B}\|\langle 001\rangle$ in (c). b) Experimental (points) and calculated (solid lines) angular variation in a {110} plane of the EPR transitions attributed to the Fe^+(III) center. The unmarked transitions correspond to the Fe^{3+} centers.

In the 200–290 K annealing range, several additional EPR lines with lower intensity have been observed close to the EPR transitions of the Fe^+(III) center (Fig. 2). These lines have been attributed to another electron-trapped Fe^+ center, called Fe^+(IIIa).

The angular variation in a {110} plane of the EPR lines of the Fe^+(IIIa) center is similar to the one of the Fe^+(III) center, suggesting a similar local monoclinic symmetry. Moreover, the spin Hamiltonian parameters of the Fe^+(IIIa) center, presented in Table I, are also very close to those of the Fe^+(III) center.

C. EPR properties of the Fe^+(IV) center

In the EPR investigations of the Fe^+(I) center, which is characterized by a very high thermal stability, the irradiated samples were usually annealed for 5 to 10 min at 700 K and quenched at RT.[5] One could thus bleach out all other paramagnetic centers produced by irradiation, without sensibly changing the concentration of the resulting Fe^+(I) centers. After several such cooling-irradiation-heating cycles, the EPR measurements at very low temperatures revealed, in addition to the lines of the Fe^+(I) center, a set of lines. These lines, with a lower intensity compared to those of the Fe^+(I) center, did exhibit a well-resolved structure consisting of four equidistant components with quasi-equal intensity (Fig. 4). This four-component structure, which is visible only at $T<10$ K, while the EPR lines of the Fe^+(I) center are visible up to 120 K,[5] is attributed to a paramagnetic center called Fe^+(IV). At $T=5$ K and below, its EPR lines begin to saturate for microwave powers of a few mW.

The angular variation of the EPR spectrum in a {110} plane is represented in Fig. 4(b) by full and open circles for the transitions of the Fe^+(IV) and Fe^+(I) centers, respectively. The angular variation of the Fe^+(IV) center is described (solid lines) by the simple spin Hamiltonian with tetragonal symmetry around one of the $\langle 100\rangle$ directions

$$H_S = \mu_B g_{//} B_z S_z + \mu_B g_\perp (B_x S_x + B_y S_y), \qquad (2)$$

where $g_\parallel = 2.097$, $g_\perp = 4.859$, and the effective spin $S=1/2$.

It seems very likely that the equally intense four-line structure represents a superhyperfine (SHF) structure due to the magnetic interaction between the paramagnetic electron spin and a neighboring nucleus with nuclear spin $I=3/2$ and natural abundance very close, or equal to 100%. The analysis of the EPR spectra presented in Fig. 4 yields the principal values of the SHF tensor $|A_\parallel| = 149.7$ MHz and $|A_\perp| = 278.9$ MHz. These values can be related[12] to the isotropic

TABLE I. EPR parameters of the electron trapped Fe^+-type centers in chlorinated $SrCl_2$:Fe crystals. In the case of the monoclinic centers, the z and x axes are tilted in the (110) plane with an angle α.

Center	S	g_x [1−10]+α	g_y [110]	g_z [001]+α	α (°)	D (GHz)	k	Annealing temp. (K)
Fe^+(I)[a]	3/2	$g_\perp = 4.175$ ±0.003		2.000 ±0.009	0	121.5 ±0.5		>700
Fe^+(II)[a]	1/2	$g_\perp = 5.211$ ±0.004		2.020 ±0.009	0		0.81	<250
Fe^+(IIa)[b]	1/2	5.144 ±0.004	5.268 ±0.004	2.013 ±0.009	2.1 ±0.1		0.81	<250
Fe^+(IIIa)[c]	1/2	5.635 ±0.005	4.815 ±0.005	1.98 ±0.01	3.0 ±0.2		0.81	<290
Fe^+(III)[c]	1/2	5.823 ±0.004	4.624 ±0.004	1.980 ±0.009	3.0 ±0.1		0.81	>300
Fe^+(IV)[c]	1/2	$g_\perp = 4.859$ ±0.004		2.097 ±0.009	0		0.605	>700

[a]See Ref. 5.
[b]See Ref. 8.
[c]This work.

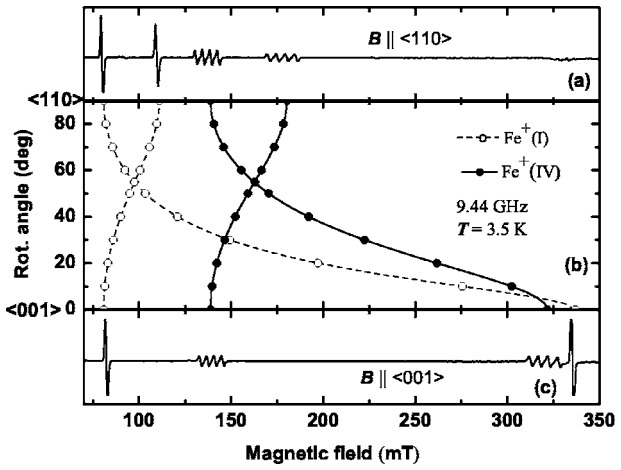

FIG. 4. X-band EPR spectra of a $SrCl_2$:Fe crystal x-ray irradiated at 80 K and annealed for 5 min at 700 K, for $\boldsymbol{B}\|\langle 110\rangle$ in (a) and $\boldsymbol{B}\|\langle 001\rangle$ in (c). (b) Experimental (open and full circles) and calculated (dashed and solid lines) angular variation in a {110} plane of the EPR transitions attributed to the Fe^+(I) and Fe^+(IV) centers, respectively.

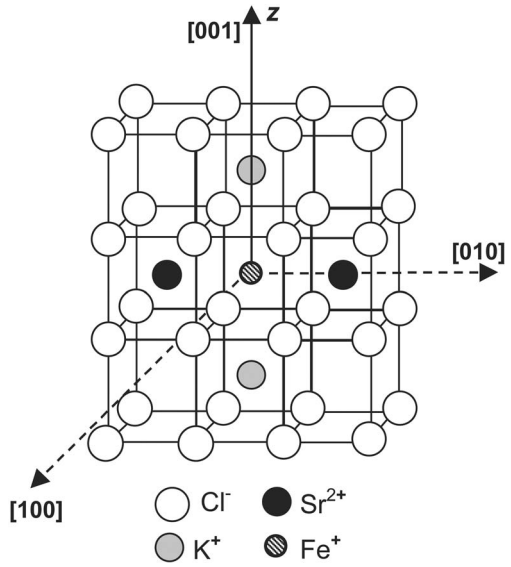

FIG. 5. The most probable structural model of the Fe^+(I) center in $SrCl_2$:Fe (see Ref. 6).

and anisotropic SHF constants a and b by the formulae:

$$A_{\|} = a + 2b, \quad A_{\perp} = a - b. \tag{3}$$

It results in either $a=235.8$ MHz and $b=-43.1$ MHz, if $A_{\|}>0$ and $A_{\perp}>0$, or $a=-235.8$ MHz and $b=43.1$ MHz, if $A_{\|}<0$ and $A_{\perp}<0$; either $a=142.9$ MHz and $b=-136$ MHz, if $A_{\|}>0$ and $A_{\perp}<0$, or $a=-142.9$ MHz and $b=136$ MHz, if $A_{\|}<0$ and $A_{\perp}>0$.

IV. STRUCTURE OF THE Fe^+- AND Fe^{3+}- TYPE CENTERS

A. The axial Fe^+-type electron-trapped centers

As shown by the previous EPR and electron-nuclear double resonance (ENDOR) studies, although the electron-trapped Fe^+(I) and Fe^+(II) centers, which are produced by low-temperature irradiation, both exhibit $\langle 001\rangle$ axial local symmetry, the observed transitions belong to different ground electron spin states, resulting from the different atomic structure of the corresponding defects.[5] Thus, the Fe^+(I) center consists of an eight-fold coordinated Fe^+ ion in an $S=3/2$ ground state, with D_{4h} site symmetry. In the most probable model (Fig. 5), two monovalent K^+ impurity ions are proposed to be symmetrically situated at the two opposite nearest-neighbor Sr^{2+} sites relative to the Fe^+ in an interstitial position.[6] Unfortunately, neither EPR, nor ENDOR could give direct proof of the presence of the cation impurities. In the case of the Fe^+(II) center, the Fe^+ ion was found to be four-fold coordinated as a result of a strong intrinsic off-center displacement of the Fe^+ ion along an $\langle 001\rangle$ axis, very close to the center of the face of the cube formed by the eight nearest Cl^- ligands (Fig. 6), which is intersected by this axis. This new four-fold coordination of the Fe^+ ion yields an $S=1/2$ ground state.[7] It should be mentioned here that the available EPR and ENDOR spectral data did not offer sufficient information to conclude on the location of the precursor Fe^{2+}(II) ion, in either a cationic substitutional site or an empty interstitial site.

The Fe^+(IV) center is different from all other Fe^+-type centers in what concerns its production properties and the presence of a large quasi-isotropic SHF structure (Fig. 4). Otherwise, it exhibits a similar $\langle 001\rangle$ axial (tetragonal) symmetry and g-component values close (Table I) to those of the Fe^+(II) center. Moreover, exactly the same g-values and the absence of high-field lines from transitions inside an

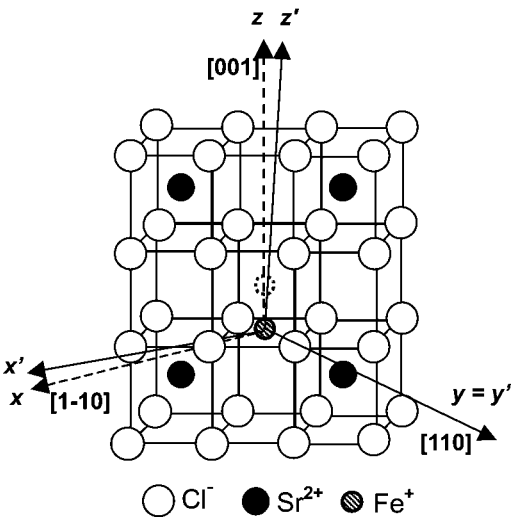

FIG. 6. Structural models of the Fe^+(II) and Fe^+(IIa) centers in $SrCl_2$:Fe. The small tilting in the (110) plane of the x' and z' principal axes of the $\vec{g}$-tensor of the Fe^+(IIa) center, attributed to the presence of a neighboring Cl^- interstitial (not shown in the figure), is somehow exaggerated for illustration purposes. The principal axes of the $\vec{g}$-tensor of the Fe^+(II) center are represented by x, y, and z. The dotted circle indicates the originating site of the precursor Fe^{2+} ion.

$S=3/2$ state have been observed in both X and Q bands. Consequently, one should also consider an $S=1/2$ state as the ground state for the Fe^+(IV) center.

Assuming a Kramers doublet as the ground state (by considering the Fe^+ ion situated close to the center of a square formed by four nearest Cl^- ligands), as in the case of the tetragonal Fe^+(II) center,[5] Tinkham's formula[13]

$$g_x + g_y + g_z = 10 + 3k \tag{4}$$

yields a $k=0.605$ value, resulting in an unusually high covalency compared to the other Fe^+ centers in $SrCl_2$ (Table I). This observation is, however, in agreement with the presence of the four-component SHF structure, which can be accurately described by the magnetic interaction with an $I=3/2$ nucleus associated with a spin delocalization onto a neighboring ion. The most probable nuclei responsible for this interaction can be either ^{23}Na ($I=3/2$, 100% abundance, and $g_N=1.47839$) or ^{39}K ($I=3/2$, 93.26% abundance, and $g_N=0.26099$), both being present as unintentional impurities in concentrations of about 100 ppm in the $SrCl_2$ starting material. In the latter case, there is another natural isotope ^{41}K with the same nuclear spin ($I=3/2$). However, due to its lower natural abundance (6.73%) and smaller nuclear moment ($g_N=0.14325$), the EPR line shape simulation, which includes contributions from both potassium isotopes, is practically undistinguishable from the simulation considering only the predominant ^{39}K isotope. It is therefore impossible to distinguish solely from EPR data, which one of the two most likely Na^+ or K^+ impurity ions is involved in the structure of the Fe^+(IV) center.

The presence of a chlorine anion next to the Fe^+ along a $\langle 001 \rangle$ axis is expected to be energetically unstable, because even for a substitutional M^{3+}- interstitial Cl^- cluster, which is supposed to exhibit a $\langle 001 \rangle$ symmetry favored by the electrostatic attraction, it was calculated[14] that the nearest-neighbor (NN) position of the interstitial is less stable than the next-NN position particularly in $SrCl_2$ crystals, due to the large lattice parameter. However, we still analyzed the possibility that the observed SHF structure originates from the magnetic interaction with a neighboring Cl nucleus. Including the two natural isotopes, ^{35}Cl (75.77%, and $g_N=0.5479157$) and ^{37}Cl (24.23%, and $g_N=0.4560820$), both with $I=3/2$, the simulation of the EPR line shape results in an equidistant four-line structure with unequal intensities, which does not reproduce the observed SHF structure with four equidistant equally intense components (Fig. 7). Moreover, it is hard to understand how the observed SHF interaction with such a neighboring Cl nucleus, which could be situated at a minimum distance of $a_0/4$ from the Fe^+ ion in the Fe^+(IV) center, can be one order of magnitude larger than the interaction with the four neighboring Cl nuclei (Table II), surrounding the Fe^+ ion in the Fe^+(II) center, situated at $a_0\sqrt{2}/4$ from the Fe^+ ion, where a_0 is the $SrCl_2$ lattice constant.[7]

Thus, from the analysis of the EPR data alone, one concludes that the Fe^+(IV) center consists of a Fe^+ ion, off-center displaced along an $\langle 001 \rangle$ axis, interacting with a NN

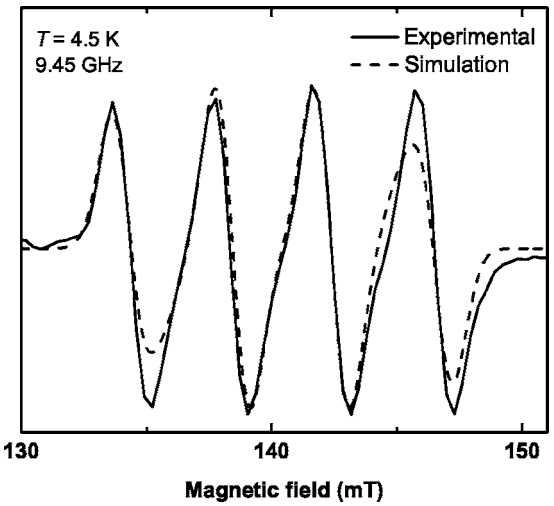

FIG. 7. Observed SHF structure of the $g_\perp$ line from the Fe^+(IV) center for $\boldsymbol{B} \| \langle 001 \rangle$ (solid line) and the best line shape fitting which can be obtained assuming an interaction with a neighboring chlorine nucleus with individual linewidth $\Delta H=0.82$ mT, considering the presence of both ^{35}Cl and ^{37}Cl isotopes with corresponding natural abundances (dashed line). The experimentally observed line shape can be accurately fitted assuming an interaction with a ligand nucleus with ~100% abundance, $I=3/2$ nuclear spin, and $\Delta H=0.82$ mT linewidth.

M^+ monovalent cationic impurity ($M^+=Na^+$ or K^+), situated on the tetragonal axis, either in the nearest empty interstitial [Fig. 8(a)] or in the cationic site [Fig. 8(b)], depending on the originating site of the Fe^{2+} precursor ion. The electrical neutrality of such a Fe^+ - M^+ pair could also explain its extremely high thermal stability.

A better insight into the nature of the neighboring M^+ impurity ion with $I=3/2$ results from a semiquantitative analysis of the experimental SHF parameters using the calculated hyperfine parameters.[15] In such an analysis, we shall consider that in the case of the Fe^+(IV) centers the charge transfer of about 40% (for $k=0.605$) to the neighboring ions takes place in a first rough approximation, mainly to the M^+ impurity ion and to the four NN Cl^- ligands. In the former case, the charge transfer is responsible for the observed four-

TABLE II. SHF parameters of the axial Fe^+-type electron trapped centers in chlorinated $SrCl_2$:Fe crystals. The principal axes of the SHF tensors are defined in the cited references.

Fe^+(I)[a]	Fe^+(II)[b]	Fe^+(IV)[c]
$A_x=2.55$ MHz	$A_x=5.98$ MHz	$\lvert A_\perp \rvert=278.9$ MHz
$A_y=5.78$ MHz	$A_y=11.42$ MHz	$\lvert A_\parallel \rvert=149.7$ MHz
$A_z=9.37$ MHz	$A_z=18.91$ MHz	
$\theta_A=7°$	$\theta_A=2°$	

[a]See Ref. 6. Parameters of the SHF interaction with first shell ^{35}Cl ligands.

[b]See Ref. 7. Parameters of the SHF interaction with first shell ^{35}Cl ligands.

[c]This work. Parameters of the SHF interaction with the $I=3/2$ nucleus of a neighboring M^+ ion.

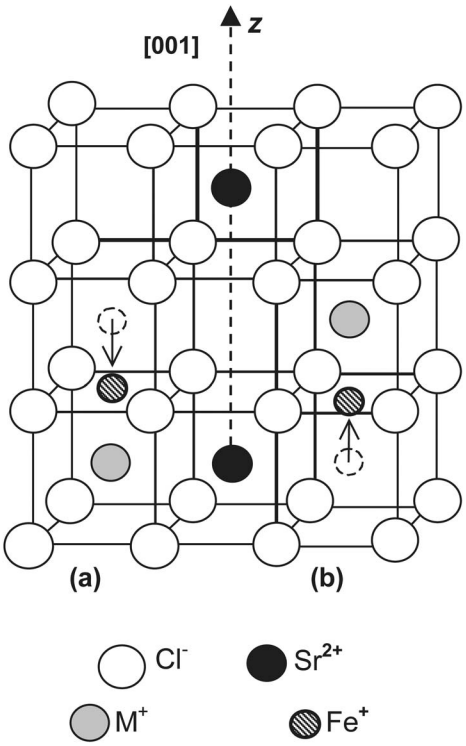

FIG. 8. The possible structural models of the Fe^+(IV) center in configurations resulting from the off-center displacement of the Fe^+ ion from: (a) The substitutional site, and (b) the interstitial site. The precursor Fe^{2+} sites are indicated by dotted circles.

component splitting. In the latter case, this results in an inhomogeneous line broadening. It is thus expected that the EPR linewidth of the Fe^+(IV) and Fe^+(II) centers to be comparable, as in both cases the paramagnetic Fe^+ ion is off-center displaced in a similar Cl^- four-fold coordinated site. Indeed, at low temperatures, the intrinsic EPR linewidth of both centers varies with orientation between 1.3 mT and 1.7 mT. Considering the observed ~20% charge transfer in the Fe^+(II) center (for $k=0.81$) to be mainly at the four nearest Cl^- ligands, one thus obtains that in the case of the Fe^+(IV) centers the remaining 20% charge transfer takes place at the M^+ impurity ion. Considering the isotropic SHF contribution of the fully localized 3*s* electron at the sodium atom of 927.1 MHz,[15] one obtains for a 20% delocalization a value of approximately 185 MHz which compares quite well, considering the very rough approximation, with the two possible experimental values of 235.8 MHz and 142.9 MHz.

A similar evaluation in the case of the K^+ impurity ion yields a value of approximately 45 MHz, too small as compared with the experimental data. Thus, it seems that M^+ is most likely a Na^+ ion.

B. The monoclinic Fe^+-type centers

Close to the EPR transitions of the Fe^+(II) center, several satellitelike lines have been observed at very low temperatures, which were attributed to another electron-trapped Fe^+ center, called Fe^+(IIa).[8] This monoclinic center, with an effective $S=1/2$ electron spin, which is also produced at low temperature, seems to be a Fe^+(II) center perturbed by some weakly interacting neighboring defect, resulting in the small monoclinic distortion of the original tetragonal deformation along an ⟨001⟩ axis. The monoclinic distortion is observed as a rhombic distortion along the perpendicular [110] and [1 −10] axes and a small tilting of the local *z* and *x* axes from the corresponding [001] and [1−10] directions in the (110) plane (Fig. 6). As will be further shown, the structure of the Fe^+(IIa) center is related to the structure of the newly discovered Fe^+(III) and Fe^+(IIIa) centers.

The other monoclinic Fe^+(III) and Fe^+(IIIa) centers, which are produced by annealing the irradiated crystals above 200 K, exhibit effective spin $S=1/2$, which is the true electron spin ground state of both centers. Indeed, as in the case of the Fe^+(IIa) center,[7] this assumption is supported by the absence in both microwave X and Q bands, for magnetic fields as high as 1.5 T, of any other transitions which could be attributed to the same paramagnetic centers, as well as from the observation of the EPR transitions at exactly the same effective *g*-values at both microwave frequencies.

If the real electron spin is $S=1/2$, one should assume for both centers a Kramers doublet as the ground state, similar to the case of the Fe^+(II) and Fe^+(IIa) centers.[5,8] Using Eq. (4), one obtains for both Fe^+(III) and Fe^+(IIIa) centers $k=0.81$, i.e., practically the same value as in the case of the Fe^+(II) and Fe^+(IIa) centers (Table I).[5,8]

The similar electronic ground state and symmetry properties of the monoclinic Fe^+(IIa), Fe^+(III), and Fe^+(IIIa) centers strongly suggest a common basic structure derived from the Fe^+(II) center, i.e., a four-fold coordinated Fe^+ ion perturbed by some weakly interacting neighboring defect(s), responsible for the monoclinic distortion of the original tetragonal symmetry. The available EPR and ENDOR studies do not offer enough data to allow a direct identification of the neighboring entity responsible for the monoclinic distortion. However, as in the cases reported earlier of monoclinic Fe^+ and Pb^+ centers in KCl,[16,17] the tilting of the $\vec{g}$- principal axes away from the main crystallographic directions in a {110} plane by a small angle could be attributed to the presence of an interstitial Cl^- ion next to one of the neighboring Cl^- ligands surrounding the Fe^+ ion. The presence of a neighboring cation has to be excluded, because only an anion interstitial can explain the monoclinic deformation in a {110} plane. The presence of several monoclinic Fe^+ centers with similar symmetry properties and different *g*-components remains to be explained.

C. The Fe^{3+}-type hole-trapped centers

According to the results of previous EPR investigations, it seems very likely that in both hole-trapped Fe^{3+}_{cub} and Fe^{3+}_{trig} centers, which are produced during low-temperature irradiation by hole trapping at corresponding precursor Fe^{2+}_{cub} and Fe^{2+}_{trig} centers, respectively, the Fe^{3+}(Fe^{2+}) ion is situated in a substitutional cationic site. The trigonal distortion of the local crystal field, observed in the latter case, can be associated with a negatively charged defect (X^{2-}) replacing one of the eight NN Cl^- ligands.[4]

The nature of the charge-compensating defect could not be unambiguously determined from the EPR data. The presence of a neighboring molecular anion, such as SO_4^{2-}, CO_3^{2-}, etc., replacing one of the eight nearest chlorine ligands has to be excluded, because the chlorination treatment is known to be a very effective procedure in eliminating the oxygen and oxygen-containing radicals from the crystal lattice of chlorides.[18] Consequently, it has been suggested[4] that a chlorine interstitial ion is situated next to one of the nearest Cl^- neighbors, resulting in a Cl^--Cl^- di-interstitial centered on one of the neighboring anionic sites and oriented along the $\langle 111 \rangle$ axis.

V. DISCUSSION: INTERSTITIALS AND IMPURITIES IN THE STRUCTURE OF PRECURSOR Fe^{2+} CENTERS

Our EPR studies of radiation-induced paramagnetic point defects in chlorinated $SrCl_2$ crystals doped with iron have revealed the presence in the as-grown crystals of both electron and hole trapping Fe^{2+} precursor centers, which have not been observed in crystals grown under an inert atmosphere. High concentrations of the resulting Fe^+ and Fe^{3+} paramagnetic centers could be produced after relatively brief (10–20 min) x-ray irradiations at low temperatures ($T < 100$ K). Because intrinsic point defects are known to be difficult to be produced by irradiation in the $SrCl_2$ lattice,[14] and no ionic movement takes place at such low temperatures,[9,10] one expects that all observed paramagnetic defects are the result of simple electron/hole trapping at the various precursor Fe^{2+} centers. Thus, the observation of the Fe^{2+} precursor centers in the chlorinated $SrCl_2$:Fe crystals seems very likely to be related with the presence of excess chlorine as interstitial chlorine ions in the crystal lattice, in agreement with our experimental observation of a slow and continuous emanation of chlorine gas from such crystals, even in normal, RT-laboratory conditions. This is also in agreement with the known general ability of the fluorite-type crystals to incorporate relatively high concentrations of anions in interstitial positions.[19]

Moreover, in the case of the chlorinated crystals, the presence of monovalent cationic impurities in the precursor Fe^{2+} centers can explain the efficient electron trapping resulting in the Fe^+(I), and Fe^+(IV) centers. The presence of the efficient electron and hole trapping Fe^{2+} precursor centers in the chlorinated $SrCl_2$:Fe crystals is also explaining the absence of EPR transitions from both intrinsic electron- and hole-trapped F and V_K paramagnetic centers, observed after x-ray irradiation at 80 K in undoped and lightly doped $SrCl_2$ crystals.[9,20–22]

Furthermore, when the temperature is increased from 100 K to 150 K, the concentration of the resulting hole-trapped Fe^{3+}_{cub} centers is strongly decreasing, while the concentration of all Fe^+-type electron-trapped centers is increasing (Fig. 1). This behavior can be explained only if there is a source of thermally freed electrons in the crystal, such as the F^* centers, i.e., F centers perturbed by neighboring impurity alkali cations,[21] which are known[9] to decay up to 125 K. The resulting mobile electrons are either trapped at positively charged (with respect to the crystal lattice) Fe^{3+}_{cub} centers, decreasing their concentration, or at Fe^{2+} precursor centers, producing more Fe^+-type centers. The absence of an observable EPR signal from the F^*-centers at $g \sim 2$ could be explained by the overlap of the intense lines from the Fe^{3+} and/or Fe^+ centers, which are present in the same magnetic field range. One should also mention that the presence of F^* centers was reported as difficult to observe in nominally pure $SrCl_2$ samples.[22]

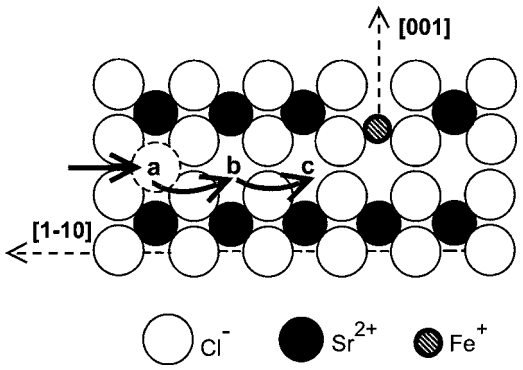

FIG. 9. Schematic model of the thermally activated movement of an interstitial Cl^- ion towards the Fe^+ ion in the (110) plane, which could explain the formation and transformation of an unperturbed tetragonal Fe^+(II) center in the sequence of monoclinic Fe^+(IIa) to Fe^+(IIIa) and Fe^+(III) centers associated with the ***a***, ***b***, and ***c*** positions of the approaching chlorine interstitial, respectively.

While the concentration of the hole-trapped Fe^{3+}_{cub} centers decreases above 100 K, the concentration of the other hole-trapped center, namely Fe^{3+}_{trig}, is not influenced by the presence of mobile electrons. The resulting thermal stability of the Fe^{3+}_{trig} centers can easily be explained with the proposed structural model.[4] Indeed, according to this model, the presence of a neighboring chlorine di-interstitial instead of a NN Cl^- ligand yields an electrically neutral Fe^{3+}_{trig} center.

The results of thermal pulse annealing experiments on $SrCl_2$:Fe crystals x-ray irradiated at 80 K, as shown in Fig. 1, offer additional interesting information concerning the presence and role of the anion interstitials in the formation and transformation of the radiolytic defects in chlorinated $SrCl_2$:Fe crystals. Thus, the tetragonal Fe^+(II) and monoclinic Fe^+(IIa) centers exhibit quite similar annealing behavior. Their decay at temperatures higher than 190 K is accompanied by the growth of two other monoclinic centers, Fe^+(III) and Fe^+(IIIa). The structural transformation of the Fe^+(II)-type centers in Fe^+(III)-type centers at temperatures higher than 190 K can be related to the motion of the interstitial chlorine ions toward the Fe^+ ion. At higher temperatures, the Fe^+(IIIa) centers transform into Fe^+(III) centers, which are stable at RT. To the best of our knowledge, there is no experimental evidence in the literature about the activation temperature of the Cl^- interstitials in $SrCl_2$. Only the theoretical activation energy of the Cl^- interstitials of about 0.9 eV has been reported so far.[14]

As shown schematically in Fig. 9, the presence of a thermally activated movement of an interstitial chlorine ion toward the Fe^+ ion could explain the conversion of the tetragonal Fe^+(II) center, which, as such, has no perturbing

chlorine interstitial in its immediate neighborhood, into the lower symmetry Fe^+(IIa) center, with the smallest rhombicity and monoclinic distortion. Further on, as the interstitial Cl^- approaches progressively closer to the Fe^+ ion in a {110} plane, the Fe^+(IIa) center is converted into the Fe^+(IIIa) and Fe^+(III) centers, which exhibit both larger rhombicity and monoclinic distortions (Table I). (The restriction of the movement of the interstitial in a {110} plane is imposed by the presence in all low symmetry Fe^+ centers of a tilting of the local z and x axes in such a plane.) Around 275 K, the Fe^+(IIIa) centers begin to transform into the Fe^+(III) centers, which exhibit the largest monoclinic distortion. The resulting Fe^+(III) centers, with the largest rhombicity (corresponding to the shortest Fe^+ - interstitial Cl^- ion separation), are the only ones left above 290 K. They are stable at RT: No significant decrease in their concentration has been observed after storing the sample at RT for several years.

The preferential final stabilization of the Cl^- interstitial in the NNN position (site ***c*** in Fig. 9), rather than in the NN position with tetragonal symmetry, is not surprising (see the corresponding discussion in Sec. IV A) and agrees with the theoretical calculations.[14]

It should be mentioned that the simultaneous presence of both tetragonal Fe^+(II) and monoclinic Fe^+(IIa) centers in about the same concentration, after low-temperature irradiation is not very clear. It could be either fortuitous, or it could mean that for some unknown reason, both Fe^{2+}(II) and Fe^{2+}(IIa) precursor centers are present in the as-grown crystals, in comparable amounts.

The thermally activated movement of the negatively charged chlorine interstitial toward the Fe^+(II) center, which consists basically of a Fe^+ ion in an off-center position, requires either a positively charged Fe^+(II) center or, at least a neutral one. This condition imposes additional restrictions on the possible structural models of the precursor Fe^{2+}(II) centers. Indeed, in the basic structural model based on EPR/ENDOR data,[5,7] a substitutional Fe^{2+} ion has trapped an electron, being displaced by an intrinsic off-center mechanism along an ⟨001⟩ axis, almost in the center of the square determined by the four nearest chlorine ligands, which intersects the direction of displacement (Fig. 6). In this model, the resulting Fe^+(II) center would be negatively charged and, thus, would not be expected to attract negatively charged chlorine interstitials.

However, it should be mentioned that the presence and movement of the interstitial chlorine ions in the neighborhood of the Fe^{2+}/Fe^+ impurity ions cannot be explained by simple Coulomb interactions. As shown in the case of alkali halides doped with monovalent impurity cations,[23] the observed movement of interstitial halide ions toward the impurities is controlled by the more subtle forces induced by the local crystal lattice distortions resulting from the presence of such impurities. This also explains why, in $SrCl_2$ doped with trivalent cations, the number of anionic interstitials is about 2.5 times larger than that required for charge compensation, as observed by neutron diffraction.[24]

One should also consider here the possible alternative interstitial localization of the Fe^{2+} ion in the Fe^{2+}(II) precursor center. Such interstitial localization of the Fe^{2+} ion in the fluorite-type lattice of $SrCl_2$ is expected to take place only if it plays the role of a charge compensating impurity for a NN substitutional M^+ cation impurity. Such a configuration could explain both the efficient electron-trapping properties of the Fe^{2+}(II) precursor center, as well as the neutrally charged character of the resulting Fe^+(II) center with respect to the crystal lattice. However, with such a structural model, it is hard to explain why the positively charged Fe^{2+}(II) precursor center does not trap chlorine anion interstitials during the crystal growth process, which would result in the observation after x-ray irradiation at 80 K of a dominant Fe^+ center with the largest monoclinic distortion.

VI. CONCLUSIONS

The analysis of the EPR spectra observed in chlorinated $SrCl_2$:Fe crystals after low-temperature ($T < 100$ K)-x-ray irradiation and after subsequent annealing at higher temperatures, resulted in the identification of several Fe^+-type electron trapped centers. Contrary to the expectancy, only in one of them, namely the Fe^+(I) center, the Fe^+ ion occupies an eight-fold cubically coordinated site. Such centers are characterized by an electronic spin $S=3/2$ and a zero-field-splitting $2D$ much larger than the Zeeman interaction (see Table I), resulting in only two EPR transitions inside the lowest and upper doublets at low and high magnetic fields, respectively.

In all other Fe^+-type centers, the Fe^+ ion is off-center displaced along the tetragonal axis, very close to the center of a square formed by the four NN chlorine ligands intersected by the displacement axis.

The pulse annealing experiments on chlorinated $SrCl_2$:Fe crystals, which have been x-ray irradiated at 80 K, resulted in the observation of the new electron-trapped Fe^+(III)-type centers with local monoclinic symmetry, related to the Fe^+(II)-type centers produced by irradiation. Their structure and transformation properties can be understood by considering the presence and thermally activated movement of neighboring chlorine interstitials (resulting from the chlorination treatment of the melt) in the {110} planes of the as-grown crystal.

The proposed structures of the electron-trapping Fe^{2+} precursors and resulting paramagnetic Fe^+ centers observed in chlorinated $SrCl_2$ crystals involve—in the case of the Fe^+(I) and Fe^+(IV) centers—the presence of neighboring M^+ alkali impurities as well. This does not seem to be the case for the hole-trapping Fe^{2+}_{trig} precursor and resulting Fe^{3+}_{trig} center, as well as for the electron-trapping Fe^{2+}(II)-type precursors and resulting Fe^+(II) and Fe^+(III)-type centers.

To the best of our knowledge, little is known so far about the presence and properties of chlorine interstitials in $SrCl_2$ crystals. Indeed, the formation of interstitials by radiolysis in $SrCl_2$ has not been reported so far. An excess of chlorine of about 3 mol % has been induced in $SrCl_2$ crystals by doping with trivalent Y^{3+} ions.[25] Furthermore, the formation of the

so-called cuboctahedral clusters of interstitial ions in ⟨110⟩ directions has been observed in coherent diffuse neutron scattering of such $(SrY)Cl_{2.03}$ crystals, in agreement with our interpretation of the formation and structure of the monoclinic Fe^{+} centers in chlorinated $SrCl_2$ crystals.

Our results confirm the general behavior of impurities in fluorite-type structures, which stabilize interstitials and enhance the coloration (radiation damage) of alkali earth fluorides by favoring the formation of impurity related defects.

ACKNOWLEDGMENTS

This work was performed under the auspices of a Flemish-Romanian collaborative scientific research project (No. BIL00/72) and with support from the Ministry of Education and Research (Program Nucleu INCDFM-PN03-180105). The Research Foundation - Flanders (FWO-Vlaanderen) is acknowledged as well for financial support in the group Project No. G.0409.02. One of us (H.V.) has been supported by FWO.

[1] A. Abragam and B. Bleaney, *Electron Paramagnetic Resonance of Transition Ions* (Clarendon Press, Oxford, 1970).
[2] J. M. De Siebenthal, D. Nicollin, and H. Bill, Chem. Phys. Lett. **58**, 317 (1978).
[3] Th. Pawlik, S. V. Nistor, and J. M. Spaeth, J. Phys.: Condens. Matter **9**, 7631 (1997), and references cited therein.
[4] S. V. Nistor, D. P. Lazar, H. Kaess, and D. Schoemaker, Solid State Commun. **104**, 521 (1997).
[5] S. V. Nistor, M. Stefan, and D. Schoemaker, Phys. Status Solidi B **214**, 229 (1999).
[6] H. Vrielinck, F. Callens, P. Matthys, S. V. Nistor, D. Ghica, and D. Schoemaker, Phys. Rev. B **64**, 024405 (2001).
[7] D. Ghica, S. V. Nistor, H. Vrielinck, F. Callens, and D. Schoemaker, Phys. Rev. B **70**, 024105 (2004).
[8] D. Ghica, S. V. Nistor, H. Vrielinck, F. Callens, E. Goovaerts, and D. Schoemaker, Phys. Status Solidi C **2**, 57 (2005).
[9] W. Hayes, R. F. Lambourn, G. Rangarajan, and I. M. Ritchie, J. Phys. C **6**, 27 (1973).
[10] S. V. Nistor, E. Goovaerts, and D. Schoemaker, Phys. Rev. B **42**, 7747 (1990).
[11] A. D. Rae, J. Chem. Phys. **50**, 2672 (1969).
[12] J. M. Spaeth, J. R. Niklas, and R. H. Bartram, *Structural Analysis of Point Defects in Solids. An Introduction to Multiple Magnetic Resonance Spectroscopy* (Springer, Berlin, 1992).
[13] M. Tinkham, Proc. R. Soc. London, Ser. A **236**, 549 (1956).
[14] P. J. Bendall, C. R. A. Catlow, and B. E. F. Fender, J. Phys. C **14**, 4377 (1981), and references therein.
[15] J. R. Morton and K. F. Preston, J. Magn. Reson. **30**, 577 (1978).
[16] E. Boesman, F. Callens, J. Haes, F. Maes, P. Matthys, and P. Moens, Solid State Commun. **77**, 931 (1991).
[17] E. Goovaerts, S. V. Nistor, and D. Schoemaker, Phys. Rev. B **28**, 3712 (1983).
[18] M. Haas, J. W. Davidson, P. H. Klein, and L. L. Boyer, J. Appl. Phys. **45**, 3959 (1972).
[19] A. B. Lidiard, in *Crystals with the Fluorite Structure*, edited by W. Hayes (Clarendon Press, Oxford, 1974).
[20] L. Matei, Solid State Commun. **9**, 1281 (1971).
[21] I. Baltog, S. Lefrant, B. Houlier, M. Yuste, J.-P. Chapelle, and L. Taurel, Phys. Status Solidi B **48**, 345 (1971).
[22] H. W. den Hartog, P. Mollema, and A. Schaafsma, Phys. Status Solidi B **55**, 721 (1973).
[23] D. Schoemaker, in *Defects and their Structure in Nonmetallic Solids*, edited by B. Henderson and A. E. Hughes (Plenum, New York, 1976), p. 173.
[24] P. J. Bendall, C. R. A. Catlow, and B. E. F. Fender, J. Phys. C **17**, 797 (1984).
[25] J. P. Goff, M. T. Hutchings, S. Hull, B. Fak, and W. Hayes, J. Phys.: Condens. Matter **4**, 1433 (1992).